Non-linearity and related features of Makyoh (magic-mirror) imaging

Ferenc Riesz

Hungarian Academy of Sciences, Research Centre for Natural Sciences, Institute for Technical Physics and Materials Science, P. O. Box 49, H-1525 Budapest, Hungary

E-mail: riesz.ferenc@ttk.mta.hu

Received

Short title: Non-linearity of Makyoh imaging

Classification numbers: 42.15.-i; 07.60.-j; 42.87.-d

Abstract

Non-linearity in Makyoh (magic-mirror) imaging is analyzed using a geometrical optical approach. The sources of non-linearity are identified as (1) a topological mapping of the imaged surface due to surface gradients, (2) the hyperbolic-like dependence of the image intensity on the local curvatures, and (3) the quadratic dependence of the intensity due to local Gaussian surface curvatures. Criteria for an approximate linear imaging are given and the relevance to Makyoh-topography image evaluation is discussed.

Published in: J. Opt. 15 (2013) 075709
http://stacks.iop.org/2040-8986/15/075709

1. Introduction

Oriental magic mirrors ('Makyoh', after their Japanese name) [1] have received much interest from the optics community since the 19th century [2-5]. Such a mirror is an essentially flat or slightly convex mirror with a backside relief pattern, which pattern translates to the polished front face as a nearly invisible surface relief during the machining of the mirror. Projecting a parallel beam onto the front surface, a reflected pattern corresponding to the back pattern appears on a distant screen due to the focusing/defocusing action of the surface relief pattern (Fig. 1) giving the illusion of transparency. An increased interest in the phenomenon arose in the 1990s because of the principle's application as a powerful topographic tool (Makyoh topography) for the qualitative visualization of the surface relief of semiconductor wafers and other nearly flat, mirror-like surfaces [2, 6-9].

Although the basic properties of Makyoh imaging are well understood through ray-tracing simulations [2, 10] and geometrical optical [3, 4] models, the interpretation of the obtained images is not straightforward.

In this paper, a pivoting issue of many physical phenomena and metrology tools, the linearity aspects of Makyoh imaging is analysed based on a geometrical optical model. In particular, the sources of non-linearity are identified, their influences are quantified, and criteria for the approximate linear imaging are given. The relevance for the visual evaluation of Makyoh-topography imaging is discussed.

2. Background

The geometrical optical model of Makyoh imaging has been described in Ref. [4]. The model is based on the works of Burkhard and Shealy who derived the illuminance of a general surface illuminated by an arbitrary extended source in a general form [11]. The Makyoh case is special because of the

closely planar surface, the nearly paraxial ray paths, the planar screen and the parallel illuminating beam. The model consists of two equations which follow directly for applying the paraxial approximation to the formulae derived in Ref. [11]:

$$\mathbf{f}(\mathbf{r}) = \mathbf{r} - 2L\nabla h(\mathbf{r}) \tag{1}$$

and

$$I(\mathbf{f}) = \frac{1}{\left|1 - 4H(\mathbf{r})L + 4K(\mathbf{r})L^2\right|}, \tag{2a}$$

or, alternatively:

$$I(\mathbf{f}) = \left|(1 - 2LC_{\min})(1 - 2LC_{\max})\right|^{-1}, \tag{2b}$$

where $h(\mathbf{r})$ is the surface height profile, $\mathbf{r}$ is the spatial co-ordinate in the mirror plane, $\mathbf{f}$ is the same in the screen plane, and L is the distance between screen and the reflecting surface; I is the image intensity relative to that produced by a flat surface, H and K are the mean and Gaussian curvatures, respectively, and $C_{\min,\max}$ are the two principal curvatures at the point $\mathbf{r}$. Unity surface reflectivity is assumed. The intensity becomes infinite if L equals either $(2C_{min})^{-1}$ or $(2C_{max})^{-1}$, that is, if the screen is in the focus of a surface area element. These infinite-intensity points of the screen constitute the caustic curve. In the present work, we exclude the caustic region, as it is not a favoured region of imaging. This also means that the absolute signs can be dropped from Eq. (2).

These equations have a physical meaning: Eq. (1) represents a mapping of the surface plane onto the image plane according to the

gradient field of the surface, while Eq. (2) gives the intensity of the image points in terms of the local curvatures of the surface. Note that the intensities are given in the image plane points **f** as mapped by Eq. (1), but are expressed with the curvatures in the surface plane points **r**.

It can be shown using a geometrical optical analysis [3] that if the surface curvatures are negligible compared to L all over the surface, the image intensity can be approximated as:

$$I(\mathbf{r}) = \frac{1}{1 - 2L\nabla^2 h(\mathbf{r})} \approx 1 + 2L\nabla^2 h(\mathbf{r}) \qquad (3)$$

that is, the image intensity variation (as compared to unity) is proportional to the Laplacian of the surface relief. Such Laplacian contrast appears in many imaging-related areas of optics and physics, such as in the shadowgraph technique [13] and mirror electron microscopy [14]; the Laplacian filter is also a common tool used in digital image processing for edge detection [15].

3. Analysis

3.1 Basic considerations

When analysing the non-linearity, $h(\mathbf{r})$ is considered as the input. It is reasonable to regard $I(\mathbf{f}) - 1$ as the output, that is the intensity difference compared to that of a flat surface, thus $h(\mathbf{r}) = \text{const.}$ (for all $\mathbf{r}$) yields a zero output. (Since only the derivatives of h are contained in Eqs. (1) and (2), any added constant is removed from h.) It is evident based on Eqs. (1) and (2) that in the general case, the imaging is non-linear. It is important to note that Eqs. (1) and (2) scale as $hL = \text{const.}$ [4], that is, the same statements regarding the linearity will refer to both h and L.

The curvatures H and K are given in a Cartesian frame (x, y) [16] as:

$$H = \frac{r(1+q^2) - 2pqs + t(1+p^2)}{2(1+p^2+q^2)^{3/2}} \quad \text{and} \quad K = \frac{rt - s^2}{(1+p^2+q^2)^2}, \tag{4}$$

where

$$p = \frac{\partial h}{\partial x}, \quad q = \frac{\partial h}{\partial y}, \quad r = \frac{\partial^2 h}{\partial x^2}, \quad s = \frac{\partial^2 h}{\partial x \partial y} \quad \text{and} \quad t = \frac{\partial^2 h}{\partial y^2}. \tag{5}$$

A main approximation of the Makyoh imaging model is that the intensity variation in the screen plane is determined by the surface curvature variations, and the influence of the local gradients on the intensities is neglected [4, 17]. Thus, p and q are dropped from Eq. (4), that is, we arrive at

$$H(\mathbf{r}) = (r + t)/2 = \nabla^2 h(\mathbf{r}) \text{ and } K(\mathbf{r}) = rt - s^2. \tag{6}$$

As r and t, as well as H are linear in $h(\mathbf{r})$, the non-linearity of imaging stems from (i) the mapping represented by Eq. (1), (ii) the nonlinear nature of Eq. (2) manifested by the quadratic term containing the Gaussian curvature $K(\mathbf{r})$, and (iii) the reciprocal expression of the intensity in Eq. (2).

The approximated version of Eq. (3) is linear. Indeed, Eq. (3) can alternatively be derived from Eqs. (1) and (2) by approximating Eq. (1) as $\mathbf{f}(\mathbf{r}) = \mathbf{r}$ and neglecting all higher-than-first-order terms in Eq. (2) [12]. That is, Eq. (3) can be regarded as the "small-signal" linear approximation of the system of Eqs. (1) and (2).

3.2 Topological mapping

The gradient-related topological mapping represents a distortion of the object's image (see figure 2). It can be quantified as the degree of image point shifts over a certain distance. A criterion of the acceptable degree of distortion can be given by fixing a lateral distance d_L over which we accept gradient changes; in other words, the image distortion (in terms of lateral shift of image points) should everywhere be smaller than d_L. That is, based on Eq. (1), the gradient $|\nabla\, h(\mathbf{r})|$ should everywhere be smaller than $d_L/(2L)$. This criterion can also be translated to image contrast for simple surfaces on a local level by combining Eqs. (1) and (2). For instance, consider a one-dimensional sine surface with spatial period k, and peak-to-peak amplitude A. The modulation M characterizing the contrast of the Makyoh image will then be $M = 4\pi^2 LA/k^2$ as follows from Eq. (2b) [18]. On the other hand, the maximum value of the gradient of the sine surface is $2\pi A/k$. Equating this to $d_L/(2L)$ yields $M = \pi d_L/k$, which represents a simple approximate formula linking the topological distortion to the image contrast. A modulation of 0.1 can be regarded a safe value for contrast discrimination [18], which translates to d_L/k ratio of ≈0.03, implying a low level of distortion. Nevertheless, this analysis is valid only on the local level, and cannot be extended to superimposed sine surfaces in the general case.

Note that this mapping is not always perceived visually as a distortion: for example, for a surface with a uniform overall curvature, the image distortion appears as a magnification. Similarly, simple cases of distortion caused by a slowly changing gradient can be removed by a mental process.

Another global feature should also be noted. In the Fourier domain, differentiation is equivalent to multiplication by the (spatial) frequency, and second differentiation to multiplication by the frequency squared. This implies a general trend: the low-spatial-frequency features (that is, global shape) will have higher effect on the slopes, causing mainly topological distortion, while, as the image intensity is related to

the second derivatives (curvatures), high-spatial-frequency features will appear with amplified intensities in the image. (In relation to this feature, we note that the height spectrum of a random surface is usually a smoothly falling monotonic curve, often following a power rule with exponent of roughly –1 to -3 [19].)

It should also be noted that, in the practice, the large-period slope changes can be easily visualized by inserting a sparse grid in the path of the illuminating beam [4] (see also figure 2).

3.3 Overall hyperbolic-like dependence

Equations (2a) and (3) reveal a fundamental property of the imaging: an overall hyperbolic-like dependence of the intensity on the curvatures. These equations follow a general form $I = 1/(1-P(\mathbf{r}))$, where $P(\mathbf{r})$ is the term containing the curvatures and L (cf. Eq. (2a)). P has two terms: the mean-curvature term is linear in h as well as in L, while the Gaussian term is quadratic. P is zero for a perfectly flat surface. P is thus the simplest representation of the surface curvatures and L. The hyperbolic-like nature in the general case means a steeply increasing relationship, reaching the caustic limit at $P = 1$. It means that the images of higher-curvature surface features are amplified further.

Figure 3 shows the $I - 1$ *versus* P curve. The curve is linear around the origo (if P is much smaller than unity).

3.4 The effects of the Gaussian curvature

The non-linearity in P is caused by the Gaussian term in Eq. (2a) through its higher-power components. This term is quadratic also in L.

To quantify this effect in Makyoh imaging, consider a light pencil reflected from a given surface point $\mathbf{r}$. Based on Eq. (2a), P can be written in a normalized form as follows:

$$P(\mathbf{r}) = L_C(1 + e - eL_c), \qquad (7)$$

where L_C stands for $2LC_{max}$. That is, L_c is a normalized L parameter, $L_C = 1$ corresponding to the caustic limit. The quantity e equals C_{min}/C_{max}, characterising the degree of the ellipticity of the local curvatures at the given point. The value of e is between –1 to 1; $e < 0$ represents saddle shape, -1 corresponding to a pure saddle shape, $e = 0$ to cylindrical and 1 to the spherical shape [20]. Note that at $e = -1$, the sign of L_C is ambiguous, since here $-C_{min} = C_{max}$. At $e = 0$, the Gaussian term vanishes, indicated by the linear dependence according to the discussion in Sec. 3.1. If $e = 0$ holds all over the surface, than it has translational symmetry. To directly assess the effect of the Gaussian curvature, it is also worth to look at P as a function of L normalized using the mean curvature as $L_H = 2L(C_{max} + C_{min}) = L_C(1 + e)$ (here, $e = -1$ is meaningless since the mean curvature would be zero). Both L_C and L_H are linear in h, not only in L, that is, the behaviour they show also reflects that of h.

Figure 4 shows P as a function of L_C and L_H, parametrized with e. The transition from linear to quadratic dependence of P is clearly displayed as L and $|e|$ increases.

The following main conclusions can be drawn:

(1) The interpretation of the images is the most straightforward in the $e = 0..1$ range (that is, cylindrical to sphere-like surface areas), or for saddle-like areas ($e < 0$) if L is small. In this regime, the intensity *versus* height dependence is monotonous.

(2) The non-linearity is the weakest for cylindrical surfaces and the strongest for saddle-shaped areas.

(3) In contrary to intuition, small image intensities (that is, $I - 1$ around zero) do not necessarily imply linear imaging, since P has an additional zero value for a non-zero L_c (or L_H) for saddle surfaces.

However, these can be distinguished from the small-signal region around zero as a small change of L induces an image intensity change of an opposite sense.

Summarizing this section, Gaussian curvature is the main source of nonlinearity, and saddle-like surfaces are less straightforward to analyze. Changing L is an efficient way of assessing the local surface shape, as saddle surface areas cause a non-monotonic *I versus L* relationship. A criterion for the monotonic region can be written as follows (from the differentiation of Eq. (7)):

$$L_c < \mathrm{sgn}(e)(1 + e)/(2e). \quad (8)$$

As the maximum of L_c is one (caustic limit, see above), this criterion is automatically fulfilled for all L_c if $e > -1/3$. Equation (8) can be regarded as a very loose condition of a quasi-linear behaviour, useful for the rough visual interpretation of Makyoh images. Namely, human vision perceives shapes and patterns in an image through intensity changes rather than absolute intensity values [21]. In this region, the superposition principle applies but with nonlinear intensity additions, but the intensity relations, thus, cues for pattern identification, are preserved.

4. Conclusions

Makyoh imaging is non-linear by nature. Basically, it can be regarded as a Laplacian operator with some added non-linearities. Changing the screen-sample distance gives a powerful tool for assessing the non-linear features; however, it should be kept as low as possible for linear and small-distortion imaging; the minimum is determined by well observable contrast. The most problematic surface areas are those of saddle-like. The gradient-related topological distortion is pronounced at low-spatial

frequency surface shapes; in the general case, this effect is difficult to handle.

Acknowledgements

This work was supported, in part, by the (Hungarian) National Scientific Research Fund (OTKA) through Grant K 68534.

References

[1] Saines G and Tomilin M G 1999 *J. Opt. Technol.* **66** 758

[2] Korytár D and Hrivnák M 1993 *Japan. J. Appl. Phys.* **32** 693

[3] Berry M V 2006 *Eur. J. Phys.* **27** 109

[4] Riesz F 2000 *J. Phys. D: Appl. Phys.* **33** 3033

[5] Gitin A V 2009 *Appl. Optics* **48** 1268

[6] Kugimiya K 1990 *J. Crystal Growth* **103** 420

[7] Blaustein P and Hahn S 1989 *Solid State Technol.* **32** 27

[8] Pei Z J, Fisher G R, Bhagavat M and Kassir S 2005 *Int. J. Machine Tools Manufacture* **45** 1140

[9] Riesz F 2004 *Proc. SPIE* **5458** 86

[10] Riesz F 2011 *Opt. Laser Technol.* **43** 245

[11] Shealy D L and Burkhard D G 1973 *Opt. Acta* **20** 287

[12] Riesz F 2006 *Eur. J. Phys.* **27** N5

[13] Verma S and Shlichta P J 2008 *Prog. Cryst. Growth Charact. Mater.* **54** 1

[14] Kennedy S M, Zheng C X, Tang W X, Paganin D M and Jesson D E 2010 *Proc. Roy. Soc. A* **466** 2857

[15] Russ J C 2007 *The Image Processing Handbook, 5th edition* (Taylor and Francis: Boca Raton)

[16] Bronshtein I N, Semendyayev K A and Hirsch K A 1997 *Handbook of Mathematics, 3rd edition* (Springer-Verlag Telos: New York)

[17] Riesz F 2000 *J. Crystal Growth* **210** 370

[18] Riesz F 2011 *Optik* **122** 1005

[19] Berry M V and Hannay J H 1978 *Nature* **273** 573

[20] Oprea J 1997 *Differential Geometry and its Applications* (New York: Prentice Hall)

[21] Pizer S M and ter Haar Romeny B M 1991 *J. Digital Imaging* **4** 1

Figure captions

Figure 1. The rough scheme of Makyoh image formation.

Figure 2. Schematic representation of the gradient-related image distortion in Makyoh imaging.

Figure 3. The image intensity *versus* $P(\mathbf{r})$ curve (see text for further explanations).

Figure 4. $P(\mathbf{r})$ as a function of (a) L_C and (b) L_H, parametrized with e (see text for details).

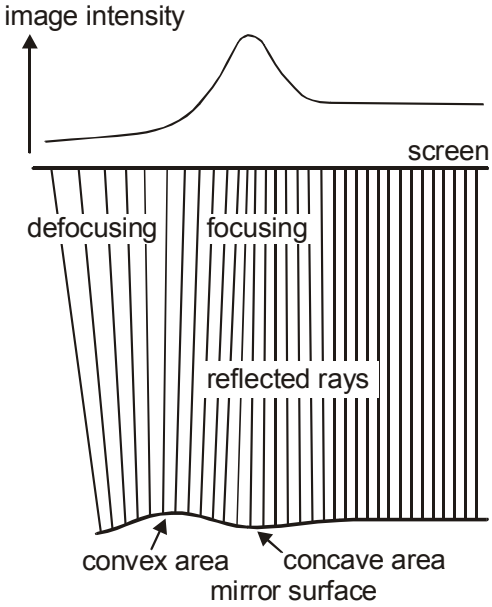

Fig. 1

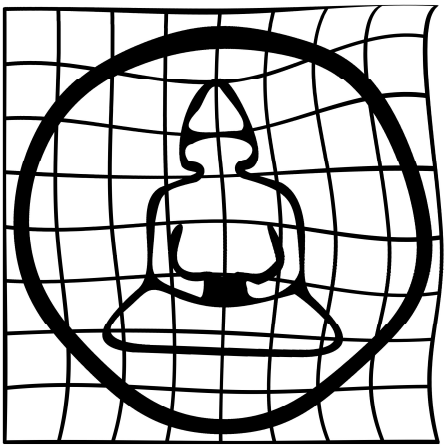

Fig. 2

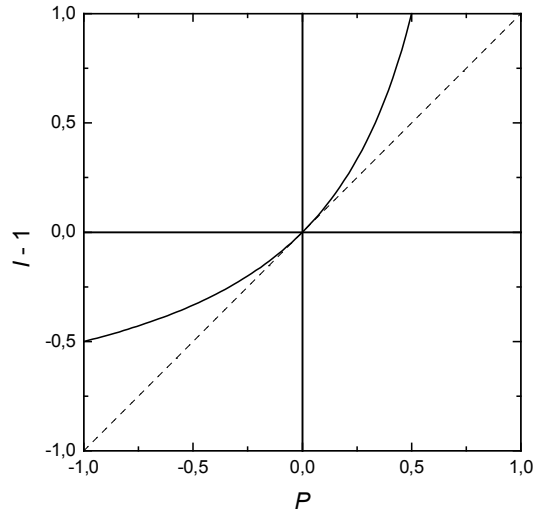

Fig. 3

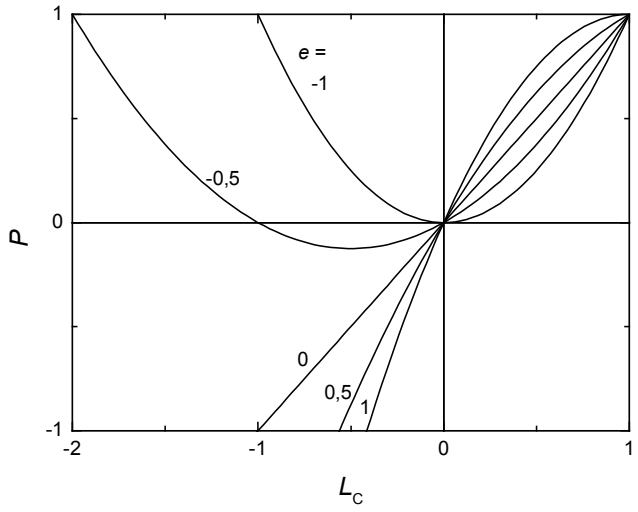

Fig. 4a

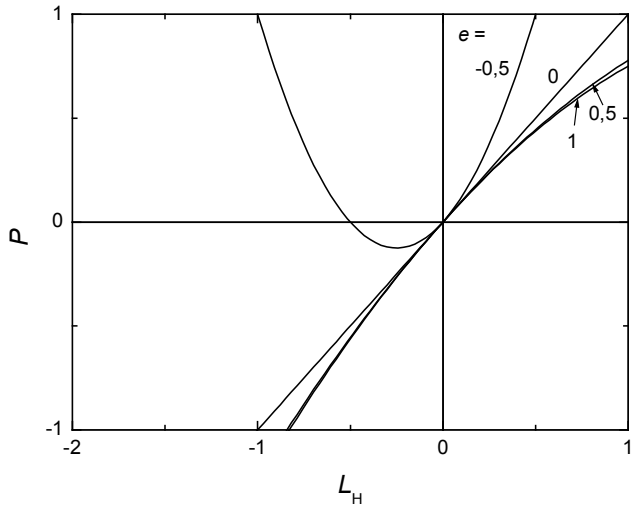

Fig. 4b